IJE TRANSACTIONS B: Applications Vol. 37 No. 08, (August 2024) 1466-1474

International Journal of Engineering

Journal Homepage: www.ije.ir

Second Order Sliding Mode Control of Three Phase Neutral Point Clamped Inverter in Stationary Frame

A. Rajabloo[a], H. Lesani*[b], S. Y. Mousazadeh Mousavi[c], S. B. Mozafari[a]

[a] *Islamic Azad Univesrity, Science and Technology Branch, Tehran Iran*
[b] *Electrical Engineering Department, University of Tehran, Tehran, Iran*
[c] *Department of Electrical Engineering, Faculty of Engineering and Technology, University of Mazandaran, Babolsar, Iran*

PAPER INFO

Paper history:
Received 08 October 2023
Received in revised form 18 November 2023
Accepted 16 December 2023

Keywords:
Master-slave Control Strategy
Harmonic Distortion
Inverter Based Microgrid
Sliding Mode Control

ABSTRACT

Grid-tied Neutral-Point-Clamped (NPC) inverters have been widely used in various applications recently. A superior control method is required to achieve the desired performance of a grid-connected NPC inverter. Accordingly, a second-order sliding mode control (SOSMC) method, which is designed in the stationary frame, is utilized for achieving this aim in this paper. The super-twisting second-order sliding mode control is used for solving the chattering problem of conventional first-order sliding mode control (FOSMC). In comparison to control methods which are applied in rotation frame, this method is not required transformation from rotating frame to a-b-c frame and vice versa and decoupling of d and q components. The Lyapunov stability analysis is used for designing of this controller. The performance of proposed method is evaluated by simulation results implemented in MATLAB/Simulink software. The performance of the SOSMC is also compared with FOSMC. The results show that the incorporation of SOSMC can improve current reference tracking of the NPC inverter in different scenarios.

***doi**: 10.5829/ije.2024.37.08b.01*

Grafical Abstract

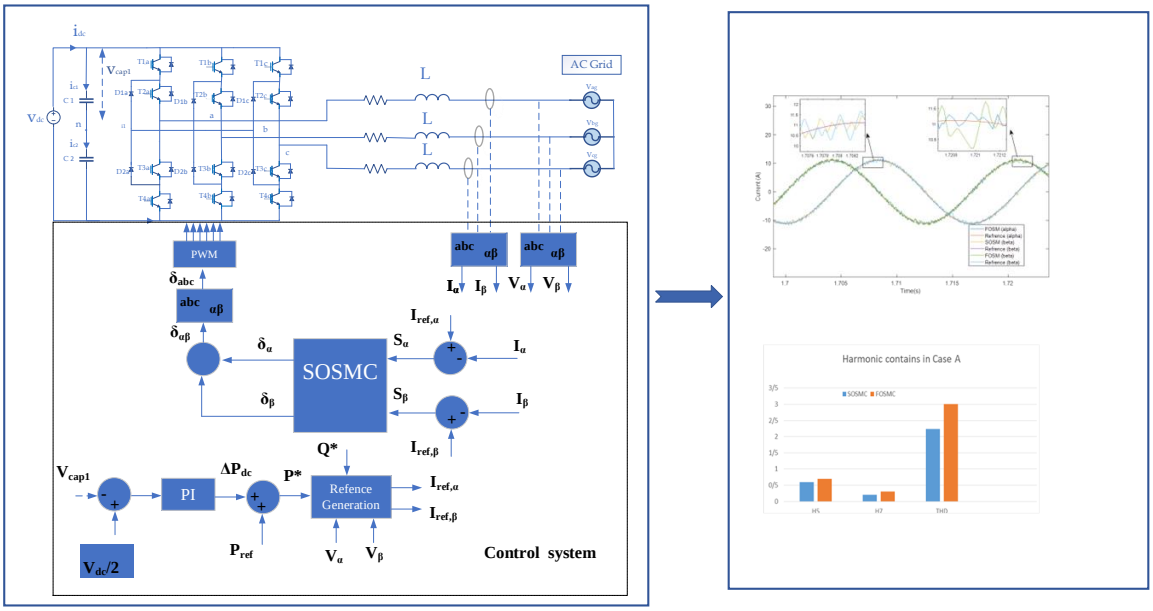

*Corresponding Author Institutional Email: lesani@ut.ac.ir (H. Lesani)

Please cite this article as: Rajabloo A, Lesani H, Mousazadeh Mousavi SY, Mozafari SB, Second Order Sliding Mode Control of Three Phase Neutral Point Clamped Inverter in Stationary Frame. International Journal of Engineering, Transactions B: Applications. 2024;37(08): 1466-74.

1. INTRODUCTION

Nowadays, multilevel inverters are widely used in different applications such as high voltage DC systems (1), interfacing inverters of distributed generation (DG) (2-5), electrical vehicles (6), solid-state transformers (7), and etc. due to their advantages, including delivering higher quality current, low voltage stress of components, higher efficiency, and their ability to operate at low switching frequency (7-11).

As DG penetration increases, current research has focused on the structure and control of grid-tied inverters; Hence, grid-tied multilevel inverters have been an attractive topic for researchers (12).

The prevalent topologies found in multilevel inverters are the Neutral-Point-Clamped (NPC) (13, 14) Flying-Capacitor (FC) (15, 16), and Cascaded H-Bridge (CHB) (17, 18). Due to the smaller size requirements of DC sources, NPC structures are an exciting option for interfacing DGs with grids (19). The control system of a grid-tied inverter should satisfy some requirements, including fast dynamic response, fixed switching frequency, DC link voltage balancing, and robustness to parameter changes (20). For the sake of these aims, different control methods are utilized for the control of grid-connected NPC inverters. The control strategies can be broadly categorized as linear and nonlinear control methodologies.The nonlinearity and uncertainty of grid-tied inverters can be controlled by using nonlinear control methods; hence nonlinear control approaches such as model predictive control (21, 22), sliding mode control (20, 23), etc., have been utilized for control of grid-tied NPC inverters. Among the nonlinear control methods, SMC has attracted more attention in the control of grid-tied NPC inverters due to its robustness against the uncertainty of the system, fast dynamic, and accurate current tracking; however, it suffers from chattering effects (24, 25). To resolve this problem, some SMC-based methods have been proposed, which can be categorized into two groups. The first category is allocated to research in which first-order SMC (FOSMC) has been used. Komurcugil et al. (26) applied SMC to a dual hysteresis band controller of NPC inverter to overcome the variable frequency problem of the hysteresis band controller and chattering effect. However, the variable frequency problem is not effectively mitigated due to changes in parameters. An SMC-based observer is incorporated by Guzman et al. (27) to reduce the states of the model; however, its implementation increases the overall complexity of the system. Although the SMC-based method proposed by Altin et al. (28) decreases the required measurement, this method suffers from the chattering effects and variable frequency problems.

Sebaaly et al. (20) introduced a PWM-based SMC control of a grid-connected NPC inverter in a rotating dq frame. Although the frequency of the proposed method is kept constant, the performance of this control scheme is dependent on the parameters of the system.

The second category of SMC-based method of NPC inverters is dedicated to the second-order SMC (SOSMC)-based method of grid-tied inverters. Ozdemir et al. (23) utilized the SOSMC approach to control a grid-connected NPC inverter which can alleviate the chattering effect and time-varying switching frequency. The methods by Ozdemir et al. (23) are implemented in the dq rotating frame, which needs computation burden for the transformation of variables from the dq to abc frame and vice versa and the decoupling and compensation process.

In this paper, a super twisting (ST)-based SOSMC is proposed for control of a three-phase grid-tied inverter in the stationary αβ. Since all of the control methods are implemented in the stationary frame, in comparison to the method proposed by Ozdemir et al. (23), the transformation of the variable from the abc frame to the rotation dq frame and vice vera is not needed which can reduce the computation burden of the controller. Additionally, this method eliminates the need for the decoupling and compensation process of d and q variables, resulting in reduced complexity and computation burden for the controller. Using the SOSMC can also eliminate the chattering effect in comparison to the FOSMC-based algorithms used and reported in literature (24-28). The controller is designed based on the Lyapunov stability theory. The main contribution of this paper is summarized as follow:

- Proposing a second order sliding control for a grid-tied NPC inverter in stationary frame
- Guarantee the stability of proposed method by Lyapunov stability analysis
- Comparison the performance of this system with FOSMC-based algorithm
- Evaluate the performance of this system in different condition

The rest of this paper is arranged in the following organization. In the second part of this paper, the general description of a three-phase grid-connected NPC inverter is presented. Section 3 is dedicated to introduce the proposed SMC algorithm for control of a grid-connected NPC inverter. Simulation results are presented in section 4. Finally, this paper is concluded in section 5.

2. GENEARL SCHEME OF THREE-PHASE CONNECTED NPC INVERTER GRID

Figure 1 depicts the structure of a three-phase NPC inverter, which is connected to the grid via an L filter. In this structure, four switches, two clamping diodes, and two split DC capacitors are utilized in each leg.

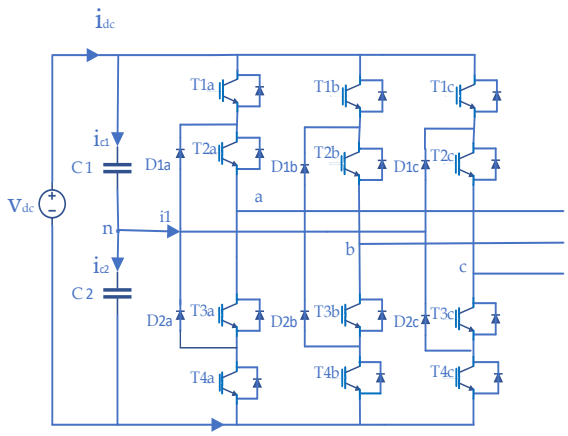

Figure 1. Structure of a NPC inverter l

As shown in this figure, the voltage stress on each power switch can be reduced by the series combination of them. The states of switches for generating a three-level phase to neutral voltage are presented in Table 1, in which the state of "On" represents the closed condition of this switch while the open state of this switch is denoted by "Off". According to this table, the switches 1, 3 as well as the switches 2, 4 operate in complementary; hence, five levels of voltages, including +Vin, +Vin/2, 0, -Vin/2, and –Vin, can be generated in line-to-line voltage.

Assuming the ideal model of switches, the dynamic model of the NPC inverter depicted in Figure 1 is written as follows in abc coordinate frame:

$$\begin{bmatrix} v_{ga} \\ v_{gb} \\ v_{gc} \end{bmatrix} = L\begin{bmatrix} \frac{di_a}{dt} \\ \frac{di_b}{dt} \\ \frac{di_c}{dt} \end{bmatrix} + \frac{1}{3}\begin{bmatrix} 2 & -1 & -1 \\ -1 & 2 & -1 \\ -1 & -1 & 2 \end{bmatrix}\begin{bmatrix} v_{a0} \\ v_{b0} \\ v_{c0} \end{bmatrix} \quad (1)$$

$$L\begin{bmatrix} \frac{di_a}{dt} \\ \frac{di_b}{dt} \\ \frac{di_c}{dt} \end{bmatrix} = \begin{bmatrix} v_{ga} \\ v_{gb} \\ v_{gc} \end{bmatrix} - \frac{v_{dc}}{2}\begin{bmatrix} \delta_a \\ \delta_b \\ \delta_c \end{bmatrix} \quad (2)$$

where δa, δb, and δc represent the control input. It should be mentioned that Equation 1 is valid if the amount of these control inputs will be in the range of [-1, 1] without saturation. In this study, the stationary frame (αβ) model is used to achieve better current tracking performance and reduce commutation burden. This model is obtained using the Clark matrix as shown in Equation 3.

TABLE 1. Switching states of three-level NPC inverter for phase x

Switching function u_x	Switching States				Output voltage of V_{xn}
	T_{1x}	T_{1x}	T_{1x}	T_{1x}	
1	On	On	Off	Off	$+V_{dc}/2$
0	Off	On	On	Off	0
-1	Off	Off	On	On	$-V_{dc}/2$

$$x_{\alpha\beta 0} = \frac{2}{3}\begin{bmatrix} 1 & -\frac{1}{2} & -\frac{1}{2} \\ 0 & \frac{\sqrt{3}}{2} & -\frac{\sqrt{3}}{2} \\ \frac{1}{2} & \frac{1}{2} & \frac{1}{2} \end{bmatrix} \quad (3)$$

The αβ stationary frame model of system presented in Equation 1 is written as:

$$L\begin{bmatrix} \frac{di_\alpha}{dt} \\ \frac{di_\beta}{dt} \end{bmatrix} = \begin{bmatrix} v_\alpha \\ v_\beta \end{bmatrix} - \frac{v_{dc}}{2}\begin{bmatrix} \delta_\alpha \\ \delta_\beta \end{bmatrix} \quad (4)$$

The controller should be designed in order to αβ stationary currents (i_α and i_β) track their references ($i_{\alpha,ref}$ and $i_{\beta,ref}$) according to the following equation:

$$i_\alpha = i_{\alpha,ref} \quad i_\beta = i_{\beta,ref} \quad (5)$$

As mentioned before, in this paper, a second order sliding mode controller is presented in αβ frame.

3. SLIDING MODE CONTROL OF THREE PHASE GRID CONNECTED NPC

The robustness of SMC against disturbances, changing system parameters, and undesired noises makes it a desirable solution for compensating for uncertainties in the system model. Although this method possesses a fast dynamic, the chattering problem is one of the drawbacks of this system. In the rest of this section, at first, the FOSMC control of a three-phase grid-connected NPC inverter is proposed. Afterward, this controller is developed by a SOSMC approach.

3. 1. First Order Sliding Mode Control Initially, a sliding surface is chosen to accomplish the controller's goal, which is current tracking. Subsequently, the control input is determined to keep the system within this specified sliding surface. In this paper, the sliding surface (Sα and Sβ) is defined as follows:

$$S_\alpha = i_\alpha - i_{\alpha,ref}\ , S_\beta = i_\beta - i_{\beta,ref} \quad (6)$$

The aim of the control is reaching to a zero-sliding surface according to the following equation:

$$\sigma = \begin{bmatrix} S_\alpha \\ S_\beta \end{bmatrix} = 0 \quad (7)$$

where σ represents the sliding surface matrix. If control variables remain on this surface, it means that each current can track its reference properly. According to Lyapunov stability, it is enough to find a definite

positive function of the sliding surface whose derivative is negative definite in order to prove that the system converges on the sliding surface and remains on its surface, which is obtained by finding those limits; hence, for stable operation following constraints must be satisfied. The P is defined as:

$$P = \frac{1}{2}\left(S_\alpha^2 + S_\beta^2\right) > 0 \ , \quad \dot{P} = S_\alpha \dot{S_\alpha} + S_\beta \dot{S_\beta} < 0, \dot{S_\alpha} S_\alpha < 0, \dot{S_\beta} S_\beta < 0$$

where Sα, and Sβ denote the sliding surface in α and β frames, respectively. The derivatives of these surfaces are represented by (S_α)˙ and (S_β). Equation 1 can be rewritten as follow:

$$\dot{S_\alpha} = \frac{1}{L} V_\alpha + \left(-\frac{V_{dc}}{2L}\right).\delta_\alpha, \dot{S_\beta} = \frac{1}{L} V_\beta + (-\frac{V_{dc}}{2L}).\delta_\beta \quad (8)$$

The control law (δ) which satisfies S ̇=0 consists of two terms according to the following equation:

$$\delta = \delta_{eq} + \delta_{st} \quad (9)$$

where, δeq is used for removing the nonlinearity of this system, while δst is utilized in order to reduce the chattering effect. The general form of Equation 9 can be expressed by the following equation:

$$\dot{S} = f + g.\delta \quad (10)$$

where f is nonlinear term of this system, while g represents the linear term of this system. For removing this nonlinear part, the following equation should be satisfied:

$$\dot{S} = f + g.\delta_{eq}=0 \quad (11)$$

According to the above equation, the δeq can be given as:

$$\delta_{eq} = \frac{-f(x)}{g(x)} = \frac{2V_\alpha}{V_{dc}} \quad (12)$$

As mentioned before, the first-order SM control cannot achieve the desired goal due to the chattering problem. In this paper, to reduce the chattering effect, the proposed method by Gao is incorporated (20, 29). To fulfill this aim, the δst is used according to the following equation:

$$\delta_{st} = -\varepsilon Syn(S) - kS \quad (13)$$

The parameters ε and k in sliding mode control represent coefficients that determine the contingency speed. Now, by replacing these coefficients in Equation 8, the limitations of control parameters for stable operation are obtained. For stable operation, it is sufficient that both coefficients are positive.

So far, the first-order sliding mode control signal has been obtained, and its limits have been determined by Lyapunov stability. In the next part, SOSMC-based control of an NPC inverter is discussed.

3. 2. Second Order Sliding Mode Control The second derivation of the sliding surface is written as follows:

$$\ddot{S_\alpha} = \frac{1}{L}\dot{V_\alpha} + (-\frac{V_{dc}}{2L}).\dot{\delta_\alpha} \quad (14)$$

$$\ddot{S_\beta} = \frac{1}{L}\dot{V_\beta} + (-\frac{V_{dc}}{2L}).\dot{\delta_\beta} \quad (15)$$

The recent equations can be expressed in the following format:

$$\ddot{s} = a + b\dot{\delta} \quad (16)$$

where, the nonlinear term (i.e. a) can be written as follows:

$$a = \begin{bmatrix} -\frac{1}{L}\dot{V_\alpha} \\ -\frac{1}{L}\dot{V_\beta} \end{bmatrix} \quad (17)$$

while the derivation of control input(δ ̇) can be presented based on super twisting sliding mode control (19):

$$\begin{cases} \delta_\alpha = -\alpha\sqrt{|S_\alpha|}Sgn(S_\alpha) - \beta \int Sgn(S_\alpha) \\ \delta_\beta = -\alpha\sqrt{|S_\beta|}Sgn(S_\beta) - \beta \int Sgn(S_\beta) \end{cases} \quad (18)$$

where α and β are control parameters that affect stability and steady-state error, respectively. As mentioned before, the stability of this nonlinear system will be guaranteed if a definite positive function of the sliding surface which satisfies the following equation is found:

$$\dot{P} = S_\alpha\left[-\frac{1}{L}V_\alpha + \frac{V_{dc}}{2L}\delta_\alpha\right] + S_\beta\left[-\frac{1}{L}V_\beta + \frac{V_{dc}}{2L}\delta_\beta\right] < 0 \quad (19)$$

By substituting Equation 19 into Equation 20, the following equation is derived:

$$\dot{P} = \frac{-V_{dc}}{2L}\left[\alpha\sqrt{|S_\alpha|}Sgn(S_\alpha) + \beta \int Sgn(S_\alpha)\right] - \frac{V_\alpha}{L} - \frac{V_{dc}}{2L}\left[\beta\sqrt{|S_\beta|}Sgn(S_\beta) + \beta \int Sgn(S_\beta)\right] - \frac{V_\beta}{L} < 0 \quad (20)$$

According to Equation 21, If α and β are determined in large values, the condition of P ̇<0 will be obtained. The performance of the controller will be enhance if α and β are determined as follows:

$$\alpha > \frac{A_M}{B_L}\ B^2 \geq \frac{4A_M B_U(\alpha + A_M)}{B_L^3(\alpha - A_M)} \quad (21)$$

where AM represent the positive bound of A. The minimum value of AM is determined as AM≥ | A | . BL and BU denote minimum and maximum amount of positive part of b (i.e., BL≤b≤ BU. a and b are the terms of the second derivative of S, which are expressed in Equation 17. These terms can be written as follows:

$$a = \frac{-1}{L}\begin{bmatrix} \dot{V_\alpha} \\ \dot{V_\beta} \end{bmatrix}\ b = \begin{bmatrix} \frac{V_{dc}}{2L} & 0 \\ 0 & \frac{V_{dc}}{2L} \end{bmatrix} \quad (22)$$

Figure 2 shows the implementation of the SOSMC in αβ stationary frame to control a grid-tied NPC inverter. According to this figure, the injected currents of the NPC inverter in αβ stationary frame (Iα and Iβ) are subtracted with their reference values (Iref,α and Iref,β) to generate

sliding surfaces according to Equation 6. Afterward, the SOSMC is applied to generate control input for this NPC inverter. Following the αβ/abc transformation, the δ angle is employed to generate pulses for the switching of NPC inverters. In order to regulate the DC voltage of the upper and lower capacitors and balance these voltages, a proportional-integrator (PI) controller is used. The PI controller's output, depicted in Figure 2 as ΔPdc, is added to the reference power (Pref) to generate P*. Afterward, by assuming the reference reactive power as Q*, the reference currents in αβ frames are obtained according to the following equation:

$$\begin{bmatrix} I_{ref,\alpha} \\ I_{ref,\beta} \end{bmatrix} = \begin{bmatrix} V_\alpha & V_\beta \\ -V_\beta & V_\alpha \end{bmatrix}^{-1} \begin{bmatrix} P^* \\ Q^* \end{bmatrix} \quad (23)$$

4. SIMULATION RESULTS

In this section, the performance of the proposed control scheme is evaluated in different scenarios using MATLAB/Simulink software. Illustrates a case study of the system shown in Figure 1. The power and control system parameters are listed in Table 2.

First, the proposed method's performance is investigated under ideal grid voltage without harmonic pollution. Afterward, Harmonic pollution is applied to the grid voltage to test control system performance in worst-case scenario. Finally, the system's performance is evaluated when the reference power is changed suddenly. The permeance of this control system is also compared with FOSMC performance.

4. 1. Case A: with Undistorted Grid Voltage

Figure 3 shows the injected currents of the NPC inverter utilizing SOSMC when the grid voltage is undistorted. The reference power, in this case, is chosen 3000 W. The harmonics contained in the injected current are listed in Figure 4. According to this table, the amount of total harmonic distortion (THD) is 2.25, and each individual harmonics is in their standard levels. These harmonic indexes are compared when FOSMC is used as the control system. This comparison shows that although the levels of low-order harmonics are closer by using FOSMC and SOSMC, the THDs are different due to high-frequency ripples when FOSMC is used as the control system.

Figure 5 shows the αβ currents of the injected current of NPC inverter by application of proposed SOSMD and FOSMD. According to this figure, it is evident that the SOSMC can track its reference more precisely.

TABLE 2. Power and control parameters

Grid voltage (V_g)	180 V Phase-Phase
Grid frequency (f)	60 Hz
Filter inductance (L)	10 mH
DC link voltage (V_{dc})	350 V
SOSMC gains (α and β)	0.65 and 1.2
Switching frequency (f_{sw})	2 KHz

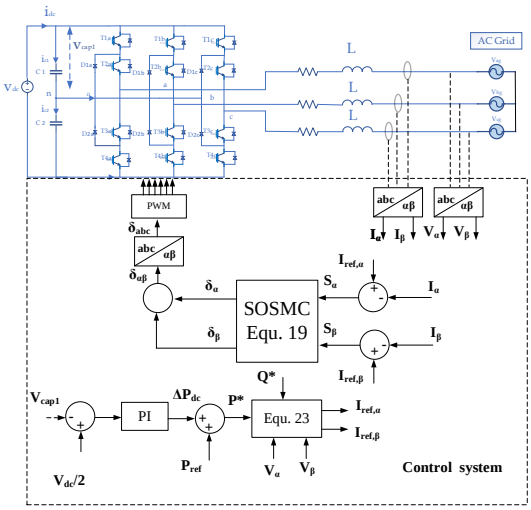

Figure 2. Control system of super twisting sliding mode control applied to a three-phase grid-connected NPC inverter

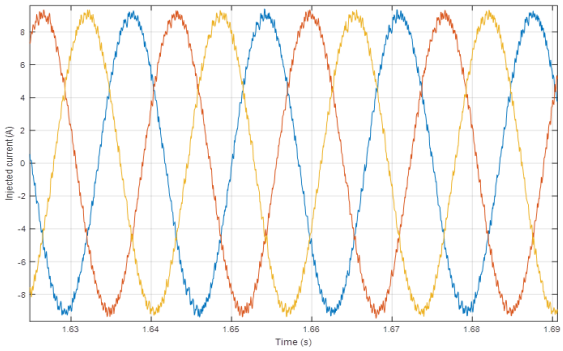

Figure 3. Injected current of grid-tied NPC in Case A by utilization of SOSMC

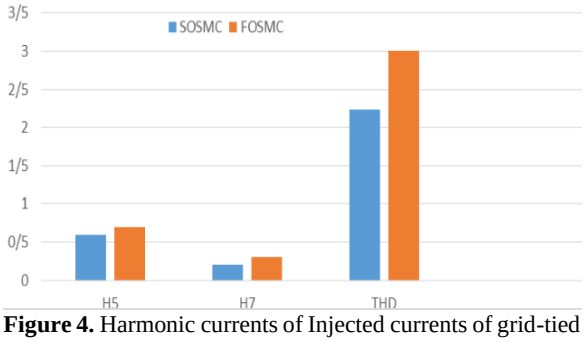

Figure 4. Harmonic currents of Injected currents of grid-tied NPC in Case A by utilization of SOSMC and FOSMC

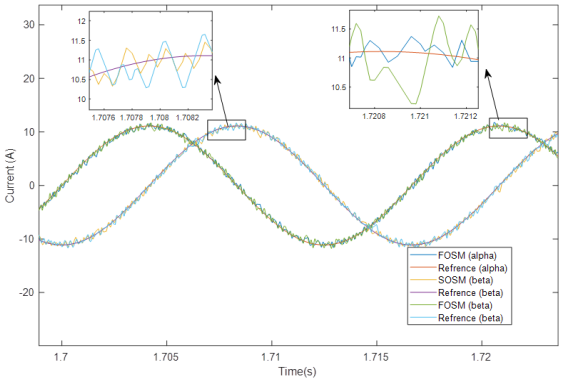

Figure 5. Injected current of grid-tied NPC in Case A by utilization of SOSMC and FOSM in αβ

Also, in order to show the superior performance of the SOSMC compared to FOSMC, three types of error indices are presented in Table 3. These indices are Integral Square Error (ISE), Integral Time Square Error (ITSE), and Integral Time Absolute Error (ITAE), which are obtained by running the simulation from t=0.5 s to t=3 s. As it is evident from this table, the SOSMC shows superior performance in all indices in comprison to FOSMC, which shows that the SOSMC can track the reference current more accurately in comparison to FOSMC.

Figure 6 shows the voltages of the upper and lower DC link capacitors (C1 and C2). According to this figure., by using the proposed control method, a voltage balance between C1 and C2 is achieved. In order to show the performance of this system in reactive power injection, the reference reactive power is considered zero (Q*=0). The current and voltage waveforms is depicted in Figure 7 for this case study. This figure. shows that the phase difference of these waveforms is zero, which can verify the performance of this system in reactive power injection. It is worth mentioning that for better depiction and comparison, the current waveform is multiplied by a coefficient in Figure 7.

4. 2. Case B: with Distorted Grid Voltage Figure 8(a) shows the injected current of the NPC inverter when

TABLE 3. Comparison of the performance of proposed SOSMC and the FOSMC in case A

Methods	Indices	I_α	I_β
FOSMC	ISE	0.1611	0.189
	ITSE	0.282	0.329
	ITAE	0.9073	0.9793
SOSMC	ISE	0.0806	0.0890
	ITSE	0.1407	0.1561
	ITAE	0.6365	0.6778

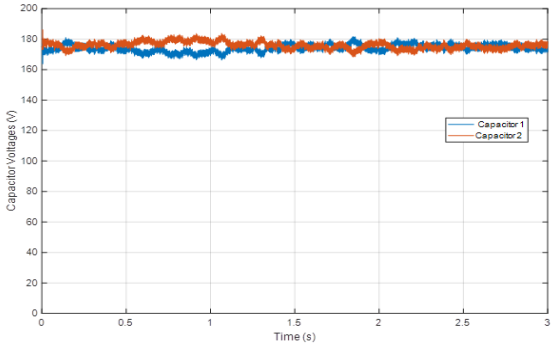

Figure 6. DC voltages of upper and lower capacitors (C1 and C2)

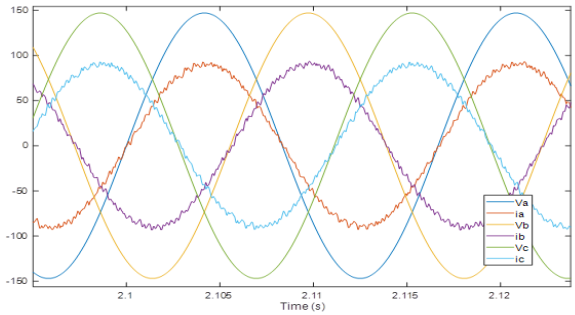

Figure 7. Voltage and current waveform with Q*=0

it is connected to a distorted grid by utilization of the SOSMC method. The voltage waveform the grid is depicted in Figure 8(b). The harmonic contains of the grid voltage and injected current of the NPC inverter are depicted in Figure 9. As shown in this figure, the THD is 2.56, and individual harmonics remain at their standard level in this condition.

4. 3. Case C: Dynamic Evaluation In order to evaluate the dynamic performance of system, a sudden chang is refrence power is happen. At first, the refrence power is assumed 2000W and it increased suddenly at t=2s. Figure 10 shows the injected currents and their refrance in αβ frame. As depicted in this figure, these surrents can track their refrences values percisely after the mentioned change.

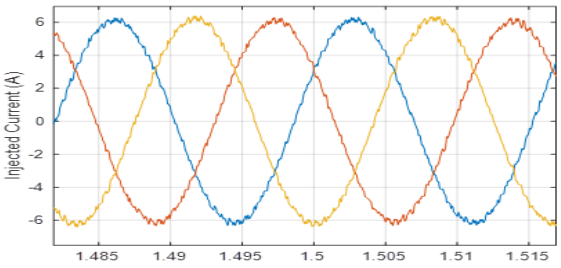

(a)

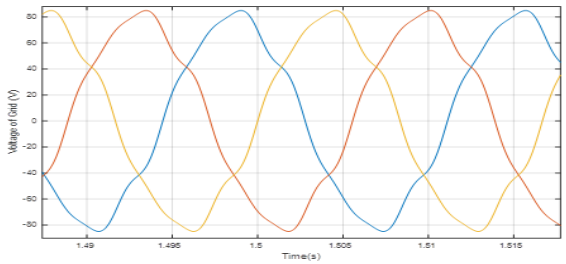

(b)

Figure 8. Voltage and current waveforms in case B by using SOSMC, (a) injected current, (b) grid voltage waveform

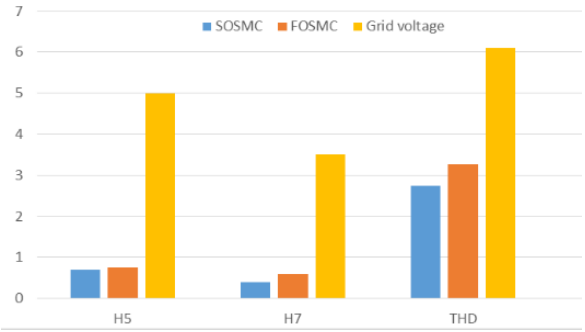

Figure 9. Harmonic currents of grid voltage and Injected currents of grid-tied NPC in Case B by utilization of SOSMC and FOSMC

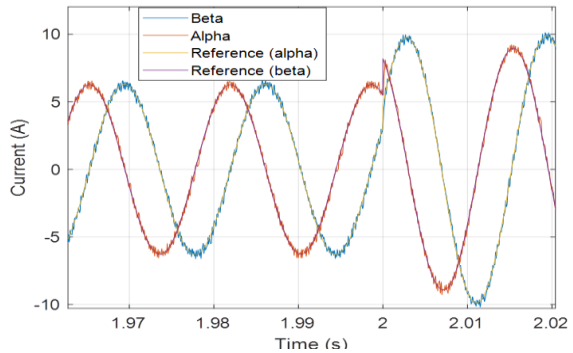

Figure 10. Injected current of the NPC inverter and their reference waveform

4. 4. Case D: Changing Parameter In this case study, the parameter of the system is changed in order to show the robustness of this method against changing parameters. In this regard, the filter inductor which is represented in Figure 2 as L is changed according to Table 4. The inductance of this filter is chosen as a sensitive parameter in order to show the change of impedance of a power network in which NPC inverter is integrated. According to this table, the controller can track the current more accurately both in the situation where the value of inductance is halved and when the value of inductance is doubled. It worth mentioning that the simulation is obtained when the grid voltage is distorted similar to Case B.

TABLE 4. Comparison of the performance of proposed SOSMC and the FOSMC in case D

Methods	Indunctance	Indices	I_α	I_β
FOSMC	L=20mH	ISE	0.1411	0. 2276
		ITSE	0.224	0.3949
		ITAE	0.8984	1.139
	L=5mH	ISE	0.6219	0.4473
		ITSE	1.097	0.7867
		ITAE	1.817	1.506
SOSMC	L=20mH	ISE	0.0403	0.0398
		ITSE	0.0707	0.06988
		ITAE	0.443	0.4461
	L=5mH	ISE	0.3142	0.3241
		ITSE	0.5488	0.5673
		ITAE	1.265	1.303

5. CONCLUSIONS

This paper presents the utilization of the SOSMC approach for control of grid-tied NPC inverter in stationary αβ. The control parameters were designed using Lyapunov stability analysis. The simulation results showed that using the SOSMC can reduce current ripple compared to using the FOSMC, which can reduce the amount of inductor filter size requirement. In addition, the simulation results showed that harmonic contents of the injected current remained at normal levels despite highly polluted grid voltages.The amount of THD was measured 2.5% when the grid voltage with THD=6.1% was applied. The system's dynamic was evaluated by a sudden 50% increase in reference current. This demonstrated the method's superior performance during the change. Finaly, the performance of SOSMC is evaluated when the filter inductance is changed, and the results show that the control method can track the refrence current acurately.

6. REFERENCES

1. Sajedi S, Farrell M, Basu M. DC side and AC side cascaded multilevel inverter topologies: A comparative study due to variation in design features. International Journal of Electrical Power & Energy Systems. 2019;113:56-70. https://doi.org/10.1016/j.ijepes.2019.05.019
2. Salehi SJ, Shmasi-Nejad M, Najafi HR. A new multilevel inverter based on harvest of unused energies for photovoltaic applications. International Journal of Engineering. 2022;35(12):2377-85. https://doi.org/10.5829/IJE.2022.35.12C.14

3. Mechouma R, Mebarki H, Azoui B. Behavior of nine levels NPC three-phase inverter topology interfacing photovoltaic system to the medium electric grid under variable irradiance. Electrical Engineering. 2018;100:2129-45. https://doi.org/10.2298/SJEE1402315M
4. Jiang J, Liang Z, Wang H. A comprehensive review on single DC source multilevel inverters for renewable energy applications. Electrical Engineering. 2023;105(6):3895-917. https://doi.org/10.1007/s00202-023-01921-4
5. Salehi SJ, Shmasi-Nejad M, Najafi HR. A new multilevel inverter based on harvest of unused energies for photovoltaic applications. International Journal of Engineering, Transactions C: Aspects. 2022;35(12):2377-85. 10.5829/IJE.2022.35.12C.14
6. Rtibi W, M'barki L, Yaich M, Ayadi M. Implementation of the ACO algorithm in an electrical vehicle system powered by five-level NPC inverter. Electrical Engineering. 2021;103:1335-45. https://doi.org/10.5829/ije.2022.35.12c.14
7. Zhang J, Zhang Y, Zhou J, Wang J, Shi G, Cai X. Control of a hybrid modular solid-state transformer for uninterrupted power supply under MVdc short-circuit fault. IEEE Transactions on Industrial Electronics. 2022;70(1):76-87. https://doi.org/10.1109/TIE.2022.3153801
8. Salehi S, Shmasi-Nejad M, Najafi HR. A New Generalized Step-up Multilevel Inverter Topology Based on Combined T-type and Cross Capacitor Modules. International Journal of Engineering. 2023;36(7):1354-68. https://doi.org/10.5829/IJE.2022.35.12C.14
9. Colak I, Kabalci E, Bayindir R. Review of multilevel voltage source inverter topologies and control schemes. Energy conversion and management. 2011;52(2):1114-28. https://doi.org/10.1016/j.enconman.2010.09.006
10. Mousazadeh Mousavi SY, Zabihi Laharami M, Niknam Kumle A, Fathi SH. Application of ABC algorithm for selective harmonic elimination switching pattern of cascade multilevel inverter with unequal DC sources. International Transactions on Electrical Energy Systems. 2018;28(4):e2522. https://doi.org/10.1002/etep.2522
11. Rodriguez J, Lai J-S, Peng FZ. Multilevel inverters: a survey of topologies, controls, and applications. IEEE Transactions on industrial electronics. 2002;49(4):724-38. https://doi.org/10.1109/TIE.2002.801052
12. Hamzeh M, Ghazanfari A, Mokhtari H, Karimi H. Integrating hybrid power source into an islanded MV microgrid using CHB multilevel inverter under unbalanced and nonlinear load conditions. IEEE Transactions on energy Conversion. 2013;28(3):643-51. https://doi.org/10.1109/TEC.2013.2267171
13. Rodriguez J, Bernet S, Steimer PK, Lizama IE. A survey on neutral-point-clamped inverters. IEEE transactions on Industrial Electronics. 2009;57(7):2219-30. https://doi.org/10.1109/TIE.2009.2032430
14. Nabae A, Takahashi I, Akagi H. A new neutral-point-clamped PWM inverter. IEEE Transactions on industry applications. 1981(5):518-23. https://doi.org/10.1109/TIA.1981.4503992
15. Escalante MF, Vannier J-C, Arzandé A. Flying capacitor multilevel inverters and DTC motor drive applications. IEEE Transactions on Industrial Electronics. 2002;49(4):809-15. https://doi.org/10.1109/TIE.2002.801231
16. Sagvand F, Siahbalaee J, Koochaki A. A Novel 19-Level Boost Type Switched-capacitor Inverter with Two DC Sources and Reduced Semiconductor Devices. International Journal of Engineering. 2023;36(2):253-63. https://doi.org/10.5829/ije.2023.36.02b.06
17. Wu B, Narimani M. Cascaded H-bridge multilevel inverters. 2017. https://doi.org/10.28991/ESJ-2022-06-01-014
18. Alemi-Rostami M, Rezazadeh G. Selective harmonic elimination of a multilevel voltage source inverter using whale optimization algorithm. International Journal of Engineering. 2021;34(8):1898-904. https://doi.org/10.5829/ije.2021.34.08b.11
19. Tavassoli F, Ghoreishy H, Adabi J, Rezanejad M. An advanced modulation technique featuring common mode voltage suppression for three-phase neutral point clamped back to back converters. International Journal of Engineering. 2022;35(11):2220-8. https://doi.org/10.5829/ije.2022.35.11b.17
20. Sebaaly F, Vahedi H, Kanaan HY, Moubayed N, Al-Haddad K. Sliding mode fixed frequency current controller design for grid-connected NPC inverter. IEEE Journal of Emerging and Selected Topics in Power Electronics. 2016;4(4):1397-405. https://doi.org/10.1109/JESTPE.2016.2586378
21. Alhosaini W, Wu Y, Zhao Y. An enhanced model predictive control using virtual space vectors for grid-connected three-level neutral-point clamped inverters. IEEE Transactions on Energy Conversion. 2019;34(4):1963-72. https://doi.org/10.1109/TEC.2019.2923370
22. Rossi M, Karamanakos P, Castelli-Dezza F. An Indirect Model Predictive Control Method for Grid-Connected Three-Level Neutral Point Clamped Converters With $ LCL $ Filters. IEEE Transactions on Industry Applications. 2022;58(3):3750-68. https://doi.org/10.1109/TIA.2022.3152463
23. Ozdemir S, Altin N, Sefa I, Zhang Z, Komurcugil H. Super twisting sliding mode control of three-phase grid-tied neutral point clamped inverters. ISA transactions. 2022;125:547-59. https://doi.org/10.1109/ACCESS.2022.3218338
24. Kelkoul B, Boumediene A. Stability analysis and study between classical sliding mode control (SMC) and super twisting algorithm (STA) for doubly fed induction generator (DFIG) under wind turbine. Energy. 2021;214:118871. https://doi.org/10.1016/j.energy.2020.118871
25. Manzanilla A, Ibarra E, Salazar S, Zamora ÁE, Lozano R, Munoz F. Super-twisting integral sliding mode control for trajectory tracking of an Unmanned Underwater Vehicle. Ocean Engineering. 2021;234:109164. https://doi.org/10.3390/jmse11091744
26. Komurcugil H, Ozdemir S, Sefa I, Altin N, Kukrer O. Sliding-Mode Control for Single-Phase Grid-Connected $\mbox {LCL} $-Filtered VSI With Double-Band Hysteresis Scheme. IEEE Transactions on Industrial Electronics. 2015;63(2):864-73. https://doi.org/10.1109/TIE.2015.2477486
27. Guzman R, de Vicuña LG, Castilla M, Miret J, de la Hoz J. Variable structure control for three-phase LCL-filtered inverters using a reduced converter model. IEEE Transactions on Industrial Electronics. 2017;65(1):5-15. https://doi.org/10.1109/TIE.2017.2716881
28. Altin N, Ozdemir S, Komurcugil H, Sefa I. Sliding-mode control in natural frame with reduced number of sensors for three-phase grid-tied LCL-interfaced inverters. IEEE Transactions on Industrial Electronics. 2018;66(4):2903-13. https://doi.org/10.1109/TIE.2018.2847675
29. Gao W, Wang Y, Homaifa A. Discrete-time variable structure control systems. IEEE transactions on Industrial Electronics. 1995;42(2):117-22. https://doi.org/10.1109/41.370376

Persian Abstract

چکیده

اینورترهای متصل به شبکه قفل‌شده نقطه خنثی در سال‌های اخیر به طور گسترده در کاربردهای مختلف مورد استفاده قرار گرفته‌اند. برای دستیابی به عملکرد مطلوب یک اینورتر قفل‌شده نقطه خنثی متصل به شبکه، یک نوع سیستم کنترل نظارتی نیاز است. به همین منظور در این مقاله از روش کنترل لغزشی مرتبه دوم که در قاب مرجع ساکن طراحی شده، استفاده شده‌است. کنترل مد لغزشی مرتبه دوم فراپیچشی برای حل مشکل پدیده چترینگ کنترل مد لغزشی مرتبه اول سنتی استفاده می‌شود. در مقایسه با روش‌های کنترلی که در قاب چرخان اعمال می‌شوند، این روش نیازی به تبدیل از قاب چرخان به قاب a-b-c و بالعکس و تجزیه به مولفه‌های d و q ندارد. برای طراحی این کنترل‌کننده از تحلیل پایداری لیاپانوف استفاده شده‌است. کارایی روش پیشنهادی با نتایج شبیه‌سازی سیستم پیاده‌سازی شده در نرم‌افزار Matlab/Simulink ارزیابی می‌شود. نتایج نشان می‌دهد که ادغام کنترل لغزشی مرتبه دوم می‌تواند ردیابی سیگنال مرجع جریان در مبدل قفل‌شده نقطه خنثی را بهبود بخشد.